Combined targeting of vascular endothelial growth factor C (VEGFC) and P65 using miR-27b-3p agomir and lipoteichoic acid in the treatment of gastric cancer

Yejia Cui[1], Shaolong Huang[1,2], Jin Cao[1], Jinjun Ye[1], Haohai Huang[3], Dan Liao[4], Yufeng Yang[5], Wanchan Chen[1], Rong Pu[1]

[1]Department of Clinical Laboratory, SSL Central Hospital of Dongguan City, Dongguan Third Clinical Hospital of Guangdong Medical University, Dongguan, China; [2]Department of Clinical Laboratory, Binhaiwan Central Hospital of Dongguan, Dongguan, China; [3]Department of Clinical Pharmacy, SSL Central Hospital of Dongguan City, Dongguan Third Clinical Hospital of Guangdong Medical University, Dongguan, China; [4]Department of Gynecology and Obstetrics, SSL Central Hospital of Dongguan City, Dongguan Third Clinical Hospital of Guangdong Medical University, Dongguan, China; [5]Department of Pathology, SSL Central Hospital of Dongguan City, Dongguan Third Clinical Hospital of Guangdong Medical University, Dongguan, China

Contributions: (I) Conception and design: Y Cui; (II) Administrative support: R Pu; (III) Provision of study materials or patients: J Ye, S Huang, H Huang, J Cao (IV) Collection and assembly of data: Y Cui, D Liao, Y Yang, W Chen; (V) Data analysis and interpretation: R Pu, Y Cui; (VI) Manuscript writing: All authors; (VII) Final approval of manuscript: All authors.

Correspondence to: Rong Pu. Department of Clinical Laboratory, SSL Central Hospital of Dongguan City, Dongguan Third Clinical Hospital of Guangdong Medical University, Dongguan 523326, China. Email: purong328073@163.com.

Background: Gastric cancer is the second leading cancer-related mortality worldwide and more effective treatment strategies are urgently needed to combat the disease. Using lipoteichoic acid (LTA) and miR-27b-3p agomir, we aimed to assess the efficacy of this combination of therapies in treating gastric cancer.

Methods: The RNA levels of miR-27b-3p, FOXO3, MET, KRAS, vascular endothelial growth factor C (VEGFC), TSC1, and P65 were analyzed by quantified-PCR (Q-PCR) and the cell viability of AGS cells was analyzed by MTT. Confirm Luciferase reporter assays were used to explore the putative miR-27b-3p binding sites and Western blot analyzed the protein level of GAPDH, VEGFC, P65, AKT, and phosphorylated-AKT (p-AKT). The level of P65 in both the cytoplasm and nucleus of AGS cells was visualized by immunofluorescence assay. Subcutaneous xenograft models of gastric cancer were established, and mice were treated with miR-27b-3p agomir, LTA, or both. Hematoxylin-eosin staining and Ki-67 immunohistochemistry analysis of tumor tissues were then performed.

Results: The results showed that the decreased expression of miR-27b-3p in gastric cancer cell lines inhibited the viability of AGS cells, and VEGFC was confirmed as the target of miR-27b-3p. In addition, ectopic expression of miR-27b-3p significantly inhibited the AKT pathway in AGS and N87 cells, and LTA suppressed the proliferation of gastric cancer cells by inhibiting the NF-κB pathway. In an established xenograft model, both miR-27b-3p agomir alone and LTA treatment alone inhibited tumor growth and treatment which combined the two showed an even stronger inhibitory effect.

Conclusions: Taken together, the combined use of LTA and miR-27b-3p agomir exhibited a synergistic effect in the treatment of gastric cancer.

Keywords: Akt; apoptosis; gastric cancer; miR-27b-3p; NF-κB; vascular endothelial growth factor C (VEGFC)

Introduction

Gastric cancer is a prevalent solid malignancy and leading cause of cancer-related mortality worldwide (1,2). Diet, infections, smoking, and obesity, especially in the presence of Helicobacter pylori, have all been implicated in facilitating the development of gastric cancer (3). Despite considerable advancements in diagnosis and treatments including surgery, chemotherapy, and radiotherapy, the prognosis of metastatic gastric cancer remains poor (4-6). Accordingly, it is necessary to discover novel clinically applicable molecular targets and more effective treatment strategies for gastric cancer.

Recently, miRNAs have been discovered to function as tumor suppressors and are closely involved the progress of many human cancers, including gastric cancer (7,8). Since miRNA levels change in cancer tissues, multiple miRNAs have been recognized as diagnostic and prognostic biomarkers for gastric cancer (9,10). The level of miR-27b was downregulated in gastric cancer tissue and its expression found to have an inverse correlation with lymph node metastasis (11). The level of miR-27b in human gastric cancer plasma was also downregulated compared with healthy controls, and the level of circulating miR-27b was significantly correlated with gastric cancer differentiation (12). The ectopic expression of miR-27b was reported to suppress gastric cancer cell proliferation by targeting receptor tyrosine kinase-like orphan receptors1 (13) and Frizzled7 (14), and the ectopic expression of miR-27b in gastric cancer was shown to facilitate multidrug resistance reversion (15). Nevertheless, the potential role of miR-27b in gastric cancer diagnosis and treatment remains elusive.

Lipoteichoic acid (LTA) is a form of teichoic acid hydrophobically anchored to a glycolipid moiety of the plasma membrane. This molecule is an amphiphile in the cell wall of Gram-positive bacteria and is a highly immunogenic glycolipid. It has many similar pathophysiological properties with lipopolysaccharide in Gram-negative bacteria (16-18). In early research, LTA was shown to promote the production of proinflammatory agonists by leucocytes and played important roles in the pathophysiology of inflammation and postinfectious sequelae (19,20). However, more studies were needed to reveal the role of LTA in immune regulatory and cancer therapy. In UV-induced skin tumors, the oral administration of LTA suppressed tumor growth once UV radiation was discontinued (17) and melanogenesis in B16F10 mouse melanoma cells was inhibited by LTA which also inhibited the expression and cellular activity of tyrosinase (18). The

combination of LTA and 5-FU showed potent antitumor effect by enhancing cell-mediated immunity (21). However, the effects of LTA on gastric cancer also remain unknown.

We proposed a combination therapy using LTA and miR-27b-3p agomir for treating gastric cancer. Our data showed that decreased expression of miR-27b-3p inhibited the viability of AGS cells by targeting vascular endothelial growth factor C (VEGFC) and inhibiting the AKT pathway. Furthermore, LTA suppressed the viability of gastric cancer cells via regulating the NF-κB pathway. Importantly, our data showed that the combined use of LTA and miR-27b-3p agomir had a synergistic anti-gastric cancer effect *in vitro* and in vivo. Our study showed the role of miR-27b-3p on VEGFC and p65 for the first time in GC by synergistic effect with LTA. These results provide a new information to support that miR-27b-3p/VEGFC might be helpful on aiding the development of novel therapeutic strategies.

We present the following article in accordance with the ARRIVE reporting checklist (available at http://dx.doi.org/10.21037/jgo-21-12).

Methods

Cell culture and treatment agents

The human normal gastric mucosa-derived cell line GES-1 and human gastric cancer cell lines (N87, BT474, MGC-803, and AGS) were obtained from the Chinese National Infrastructure of Cell Line Resource. Cells were cultured in Dulbecco's modified Eagle medium (Procell Life Science&Technology, China) supplemented with 10% fetal bovine serum (Gibco, Carlsbad, CA, USA). LTA was purchased from Bacillus subtilis (Sigma, St. Louis, MO, USA).

Cell viability assay

Wells were established and each contained 3,000 cells which were seeded, exposed to the indicated treatment, then repeatedly washed with fresh media. A 20 µL of solution of MTT (Sigma-Aldrich, USA) was then added into each well for 4 h incubation at 37 ℃ and 5% CO_2. Absorbance at 570 nm was measured by using a microplate reader (Thermo Fisher, Finland).

Quantitative real-time PCR (qRT-PCR)

RNATrizol (Invitrogen) was used to extract total RNA from cells following the protocols. mRNA was reverse

Table 1 Primers used for real-time quantitative PCR analysis

Gene	Sequence
KRAS	Forward: ACAGAGAGTGGAGGATGCTTT
	Reverse: TTTCACACAGCCAGGAGTCTT
FOXO3	Forward: CGGACAAACGGCTCACTCT
	Reverse:GGACCCGCATGAATCGACTAT
MET	Forward: AGCAATGGGGAGTGTAAAGAGG-
	Reverse: CCCAGTCTTGTACTCAGCAAC
TSC1	Forward: CAACAAGCAAATGTCGGGGAG
	Reverse: CATAGGGCCACGGTCAGAA
VEGFC	Forward: GAGGAGCAGTTACGGTCTGTG
	Reverse: TCCTTTCCTTAGCTGACACTTGT
P65	Forward: ATGTGGAGATCATTGAGCAGC
	Reverse: CCTGGTCCTGTGTAGCCATT
miR-27b-3p	RT: TAGTGTGTGTAGATAGTACGGGG
	Forward: CTACAATAAACGCGACCACG
U6	Forward: CTCGCTTCGGCAGCACA
	Reverse: AACGCTTCACGAATTTGCGT
Human GAPDH	Forward: AGAAGGCTGGGGCTCATTTG
	Reverse:AGGGGCCATCCACAGTCTTC

transcribed into cDNA by Prime ScriptTM RT reagent Kit with gDNA Eraser (Takara, Japan). miRNA was reverse transcribed into cDNA using Mir-X miRNA First-Strand Synthesis Kit (Takara, Japan). SYBR® Green (BioRad Laboratories Inc., USA) was used for qRT-PCR analysis. The thermal cycles for qRT-PCR were listed as follows: 95 ℃ for 5 min, 40 cycles of 95 ℃ for 15 s and 60 ℃ for 50 s, 95 ℃ for 15 s, 60 ℃ for 15 s and 95 ℃ for 15 s. Each reaction was performed in a technical triplicate. The relative expressions of mRNA and miRNA were normalized to GAPDH and U6, respectively. The comparative cycle threshold method and fold change was used to calculate the relative expression. The primer used is showed in *Table 1*.

Western Blot

Cells were homogenized in ice-cold lysis buffer. After being centrifuged for 5 min at 10,000 g, 15 μg protein was subjected to 10% SDS-PAGE and transferred onto PVDF membranes. The membranes were then blocked and incubated with respective primary antibodies: anti VEGFC (abcam 1:1,000), phosphorylated-AKT (p-AKT) (sigma, 1:1,500), AKT (CST, 1:1,000), P65 (abcam, 1:1,000) and GAPDH (abcam, 1:2,000). After washing, the membranes were incubated with anti-rabbit IgG-HRP (CST, 1:2,000). Bands were visualized with the enhanced chemiluminescent system (Thermo Fisher Scientific, Inc., USA). Three independent repeats of experiments were performed. The density of each band was measured using ImageJ software (National Institutes of Health, USA). GAPDH from the same sample was internal loading control.

Cell transfection

The miR-27b-3p agomir, antisense miR-27b-3p antagomir, and scrambled negative controls (NCs) were designed and purchased from Ribobio (Co Ltd., China). The MiR-27b-3p agomir sequence was: 5'-UUCACAGUGGCUAAGUUCUGC-3'; miR-27b-3p antagomir: 5'-UAGCAGCACGUAAAUAUUGGC-3'; control (5'-UUUGUACUACACAAAAGUACUG-3'. For the transfection of cancer cells, Lipofectamine™ 3000 Transfection Reagent (Invitrogen, Shanghai, China) was used.

Animals

Male Balb/c nude mice (3–4 weeks, 20–25 g) were purchased from the Animal Center of Southern Medical University. Experiments were performed under a project license (NO.: IEC2020011600012) granted by Ethics Committee of the SSL Central Hospital of Dongguan City, in compliance with SSL Central Hospital of Dongguan City guidelines for the care and use of animals. All animal experiments were conducted at the Experimental Animal Center of Southern Medical University.

Tumor xenograft experiments

We established a xenograft model by subcutaneously injecting $5×10^6$ AGS cells into the nude mice. After one week, the transplanted mice were randomly divided into four groups (n=4 per group); control, miR-27b-3p agomir (Guangzhou, China), LTA, and miR-27b-3p agomir + LTA. Mice in the control group were injected with control agomir and PBS into the implanted tumor every 4 days and those in the miR-27b-3p agomir group received a 50 nmol (200 μL) injection of miR-27b-3p agomir into the implanted tumor also every 4 days. The LTA group received

4 µmol (400 µL) of LTA per mouse by lump body injection every other day and the miR-27b-3p agomir + LTA group received 4 µmol of LTA and a 50 nmol dose of miR-27b-3p agomir per mouse. The mice were sacrificed by injection of barbiturate and suffocation in carbon dioxide.

Immunofluorescence assays

After treatment, cells were fixed in 4% paraformaldehyde and permeabilized with 0.5% Triton X-100 for 15 min. The cells were washed and blocked with 5% NGS (normal goat serum) in PBS and incubated with primary antibody overnight at 4 °C. We used P65 (1:500 Santa, USA) as the primary antibody and a secondary antibody conjugated with Alexa Fluorescence 549 (1:1,000, Invitrogen) was also used. The stained cells were visualized by a confocal microscope (OLYMPUS, Japan).

Hoechst assays

The apoptosis of cells was evaluated using a Hoechst detection kit (Roche, Germany) following the manufacturer's instructions. In brief, the cells were fixed with 3% formaldehyde, permeabilized with 0.1% Triton X-100, and incubated with Hoechst reaction mixture. The cell nucleus was then labelled with DAPI.

Luciferase assays

To confirm the 3'-untranslated regions (UTR) of VEGFC with the binding sites of miR-27b-3p, miR-27b-3p promoter reporter constructs with wild-type or mutated VEGFC-binding sites were designed and constructed by RiboBio (Guangzhou, China). Cells were transfected by Lipofectamine™ 3000 Transfection Reagent (Invitrogen, Shanghai, China). The luciferase reporter assay was performed using the Dual Luciferase Reporter Assay System (Promega, USA).

Immunohistochemistry

Tumor tissue was fixed, cut into 4 µm-thick sections, placed on glass slides, then stained with Hematoxylin-eosin. Immunohistochemistry was performed as described by Wu et al., 2016 (22) and the sections were deparaffinized with xylene. IHC was performed with primary antibodies Ki67 (CST, 1:1,000), then the sections were counterstained with hematoxylin.

Statistical analysis

All experiments were performed at least three times and P<0.05 was considered statistically significant. To determine significance between two groups, an unpaired t-test was performed and Kruskal-Wallis test was used to evaluate the differences between more than two groups using Prism statistical software package (Version 8.0, Graphpad Software Inc., CA, USA).

Results

Increased expression of miR-27b-3p in gastric cancer cell lines inhibited the viability of AGS cells

The level of miR-27b-3p in the normal gastric mucosa-derived cell line GES-1 and gastric cancer cell lines (AGS, BT474, MGC-803, and N87) was first assessed. As shown in *Figure 1A*, miR-27b-3p was significantly down-regulated in gastric cancer cell lines compared to the normal gastric mucosa-derived cell line GES-1. As AGS cells had the lowest level of miR-27b-3p compared to other gastric cancer cell lines they were chosen for follow-up experiment. This revealed miR-27b-3p expression in AGS cells to be overexpressed and inhibited, and the cell viability was then assessed. The ectopic expression of miR-27b-3p significantly inhibited the cell viability of AGS cells (*Figure 1B*) and compared with the NC, miR-27b-3p antagomir strikingly promoted the cell viability of AGS cells.

MiR-27b-3p targets VEGFC and inhibits the AKT pathway in gastric cancer cells

Target prediction algorithms using targetscan (www.targetscan.org) identified a potential binding site for miR-27b-3p in the 3'-UTR regions of KRAS, FOXO3, MET, TSC1, and VEGFC. Transfection of miR-27b-3p agomir or miR-27b-3p antagomir was then performed on AGS cells (*Figure 2A*). Our previous studies showed that miR-27b targeted VEGFC (12). As shown in *Figure 2B,C,D,E,F*, the expression of KRAS, MET, TSC1, and VEGFC was increased in AGS cells transfected with miR-27b-3p antagomir and decreased in AGS cells transfected with miR-27b-3p agomir. The VEGFC mRNA level was increased 16.9 times by transfection of miR-27b-3p antagomir compared with the NC.

The sequence of human VEGFC 3'-UTRs containing the putative binding sites of miR-27b-3p is shown in *Figure 2G*. Luciferase reporter assays were performed and showed
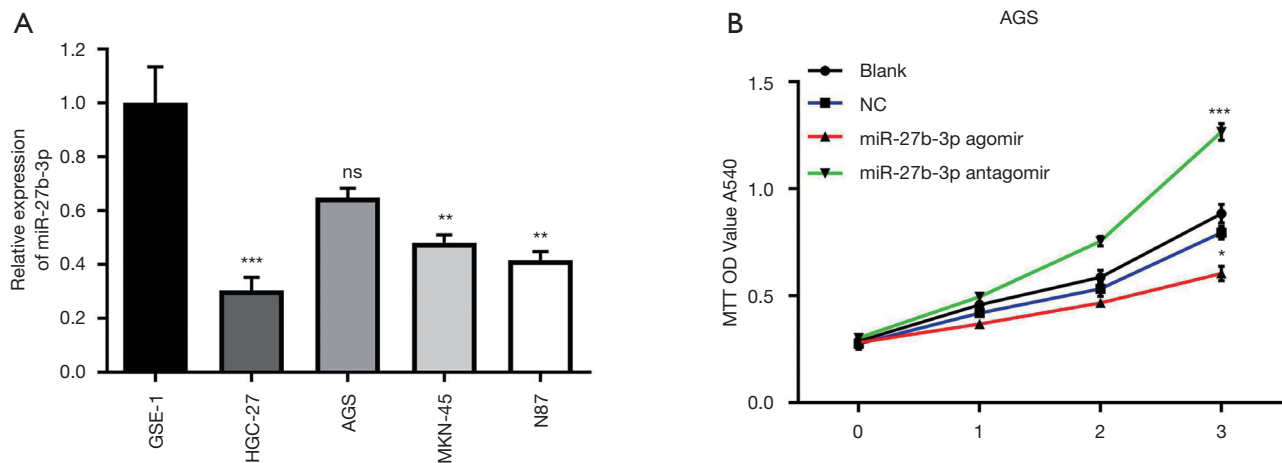
Figure 1 Knockdown of miR-27b-3p inhibited cell proliferation in AGS cells. (A) quantified-PCR (Q-PCR) analyzed the expression of miR-27b-3p in GES-1, AGS, BT474, MGC-803, and N87. (B) AGS cells were transfected by negative control (NC), miR-27b-3p agomir, or miR-27b-3p antagomir, and the cell viability was assessed by MTT. All the experiments were carried out in triplicate. *P<0.05, **P<0.01, ***P<0.001.

transfection of miR-27b-3p significantly decreased luciferase activities of the VEGFC wild-type (wt.) reporter but did not affect the mutated VEGFC (*Figure 2H*). Western blot displayed the protein level of VEGFC in AGS and N87 cells to be significantly decreased by transfection of miR-27b-3p agomir and increased by transfection of miR-27b-3p antagomir (*Figure 2H*). Previous studies reported that AKT and mTOR pathways were the major downstream regulated genes of VEGFC (23-25). In both AGS and N87 cells, the ectopic expression of miR-27b-3p inhibited the p-AKT with no effect on the expression of AKT (*Figure 2I*). In addition, the transfection of miR-27b-3p antagomir significantly increased the p-AKT in AGS and N87 cells with no effect on the level of AKT (*Figure 2I*). Taken together, miR-27b-3p targets VEGFC and inhibits the AKT pathway in gastric cancer cells.

LTA suppressed the proliferation of gastric cancer cells by inhibiting the NF-κB pathway

To investigate whether LTA inhibited the proliferation of gastric cancer cells, the AGS cells were treated with LTA. The molecular structure of LTA is shown in *Figure 3A*. As shown in *Figure 3B*, cell viability was significantly inhibited by LTA after 3 days of treatment. Previous studies reported that LTA can activate NF-κB through the recognition of TLR2 and reactive oxygen species in LTA-induced murine macrophages (26). The protein level of P65 in AGS cells

was significantly decreased by LTA treatment (*Figure 3C*) and immunofluorescence assay showed that the level of P65 in both the cytoplasm and nucleus of AGS cells was also decreased by LTA treatment (*Figure 3D*). Our results indicated that the proliferation of gastric cancer cells was suppressed by LTA through inhibition of the NF-κB pathway.

Combined use of LTA and miR-27b-3p agomir has a synergistic effect for anti-gastric cancer

To investigate whether the combined use of LTA and miR-27b-3p agomir had a synergistic anticancer effect, gastric cancer cells were treated with miR-27b-3p agomir alone or with LTA. As shown in *Figure 4A*, the cell viability of AGS and normal gastric mucosa-derived cell line (GES-1) was inhibited by miR-27b-3p agomir in a dose-dependent manner, and inhibition increased with increasing drug concentration (*Figure 4B*). The combined use of LTA and miR-27b-3p agomir showed a stronger inhibition effect on the cell viability of AGS (*Figure 4C*), and more apoptosis cells were seen (*Figure 4D*) than when either was used alone. To further investigate this synergistic effect, we established a xenograft model and found both miR-27b-3p agomir and LTA treatment alone inhibited tumor growth (*Figure 5A,B,C*). However, the combined treatment produced an even stronger inhibitory effect on tumor growth. Moreover, the combined of therapies also
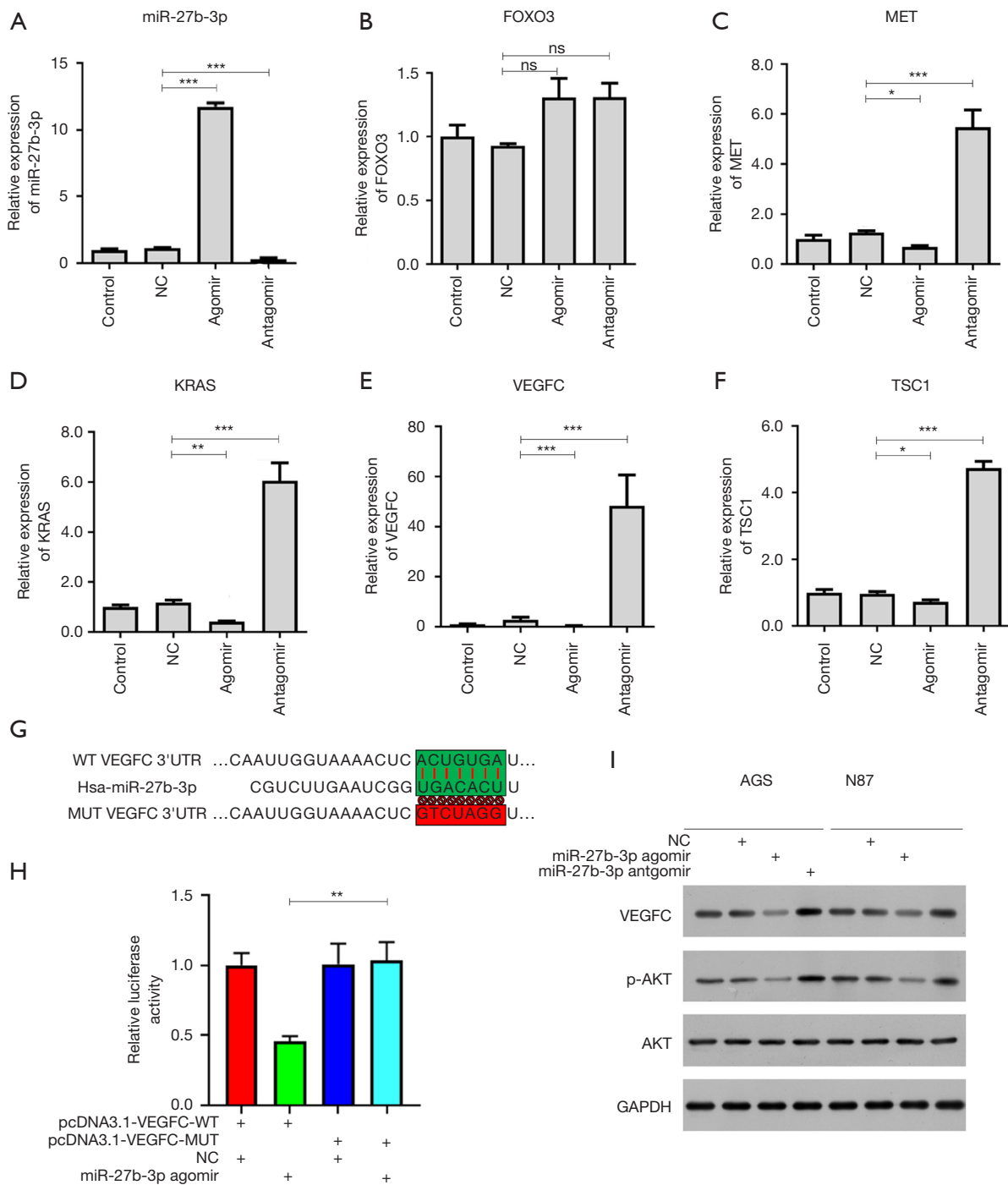
Figure 2 MiR-27b-3p targets VEGFC and inhibits the AKT pathway in gastric cancer cells. (A) AGS cells were transiently transfected with synthetic miR-27b-3p agomir, or antisense miR-27b-3p antagomir. quantified-PCR (Q-PCR) analyzed the level of miR-27b-3p in AGS cells after transfection. (B,C,D,E,F) Q-PCR analyzed the mRNA level of FOXO3, MET, KRAS, VEGFC, TSC1. (G) Schematic represents putative miR-27b-3p binding sites with VEGFC. (H) Luciferase reporter assays confirming the miR-27b-3p binding sites at 3'-UTRs of VEGFC. (I) AGS and N87 cells were transfected by negative control (NC), miR-27b-3p agomir, or miR-27b-3p antagomir, and the protein level of GAPDH, VEGFC, AKT and p-AKT was assessed by Western blot. All the experiments were carried out in triplicate. *P<0.05, **P<0.01, ***P<0.001.
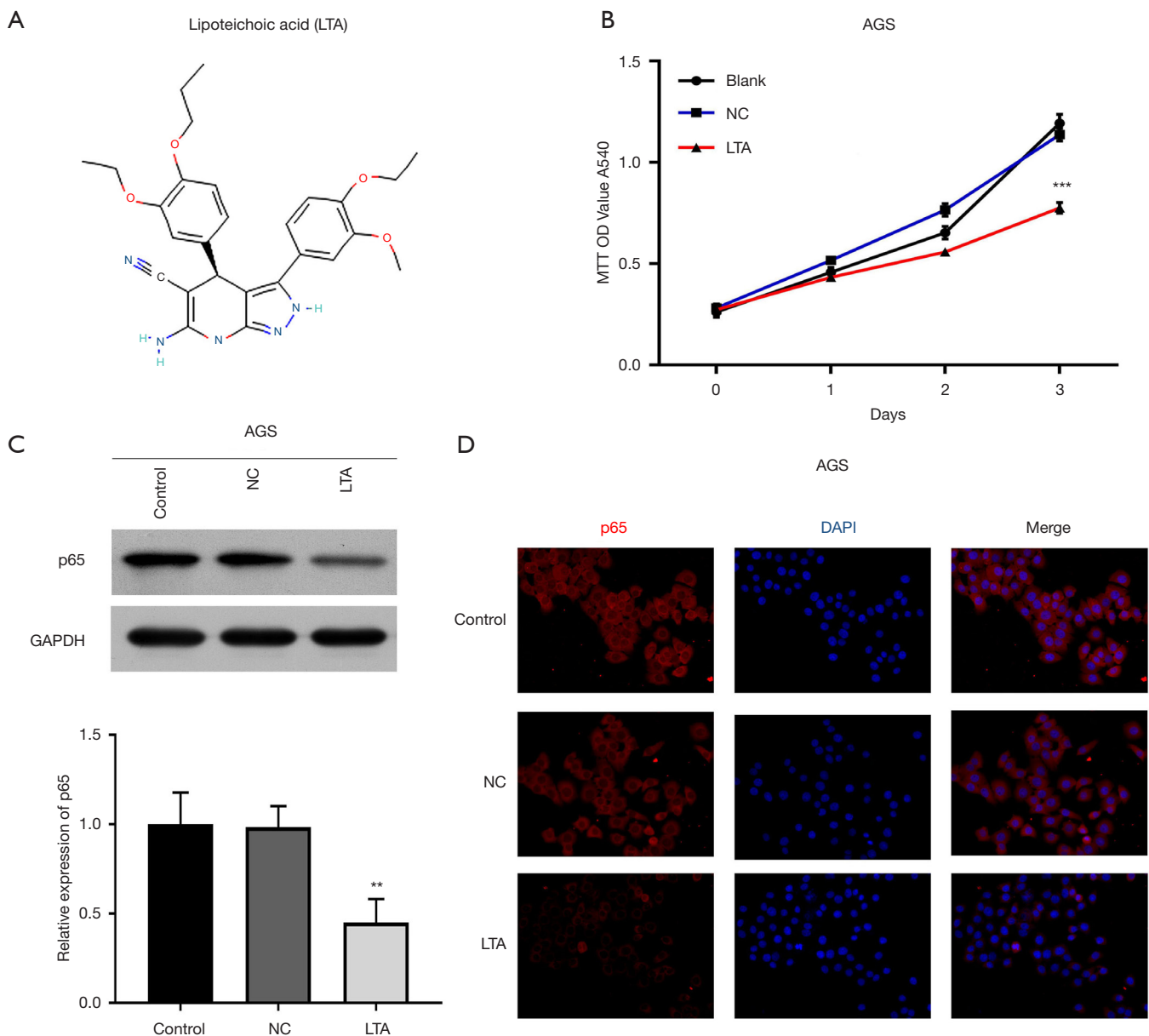
Figure 3 Lipoteichoic acid (LTA) suppressed the proliferation of gastric cancer cells by inhibiting the NF-kappa-B pathway (A) The molecular structure of LTA. (B) AGS cells were treated with LTA (4 µmol/L) for 1, 2 and 3 days. MTT assessed the cell viability. (C) Western blot analyzed the protein level of GAPDH and P65 at 3 days after LTA stimulation. (D) The level of P65 in both the cytoplasm and nucleus of AGS cells was visualized by immunofluorescence assay at 3 days after LTA stimulation. DAPI was used to stain nucleus (blue). All the experiments were carried out in triplicate. Magnification 200×. **P<0.01, ***P<0.001.

decreased immune cell infiltration in tissues and the level of proliferation marker Ki-67 (*Figure 5D*). These results indicated that the combined effects of miR-27b-3p agomir and LTA on gastric cancer were superior to the use of each alone. Collectively, the combination of therapies had a synergistic anti-gastric cancer effect which saw the inhibition of the VEGFC/PI3K/AKT pathway by miR-27b-3p and NF-κB pathway by LTA.
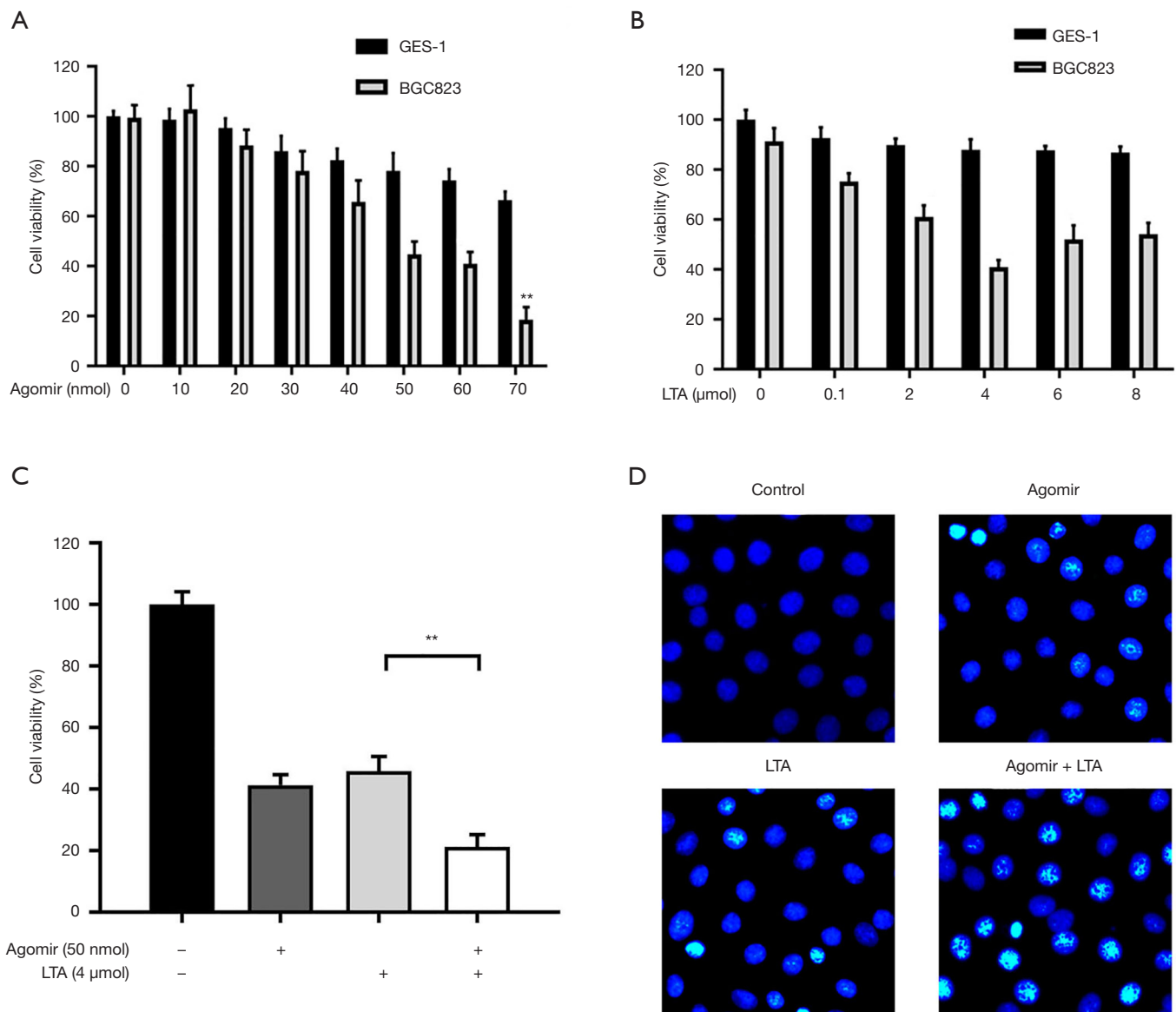
Figure 4 The combined use of lipoteichoic acid (LTA) and miR-27b-3p agomir has synergistic effect for anti-gastric cancer *in vitro*. (A) AGS cells and normal gastric mucosa-derived cell line (GES-1) were transfected by increasing concentration of miR-27b-3p agomir (0 nm–70 nmol), and MTT analyzed the cell viability. (B) AGS cells and normal gastric mucosa-derived cell line (GES-1) were transfected by increasing concentration of LTA (0–8 μmol), and cell viability was analyzed by MTT. AGS cells were treated with miR-27b-3p agomir, LTA, or both. The cell viability of AGS cells after indicated treatment was analyzed by MTT (C) and cell apoptosis was analyzed by using Hoechst assays stained with Hoechst (D). Magnification 400×. All the experiments were carried out in triplicate. **P<0.01.

Discussion

As a potent lymphangiogenic factor, VEGFC has been shown to be pivotal for lymph angiogenesis (27,28). Angiogenic VEGFC is expressed in endothelial cells, non-endothelial cell types, like cancer cells (8,29) and VEGFC was found to be highly expressed in various tumors including gastric carcinoma (28-30). In gastric carcinoma, the overexpression of VEGFC was associated with advanced regional lymph node infiltration and
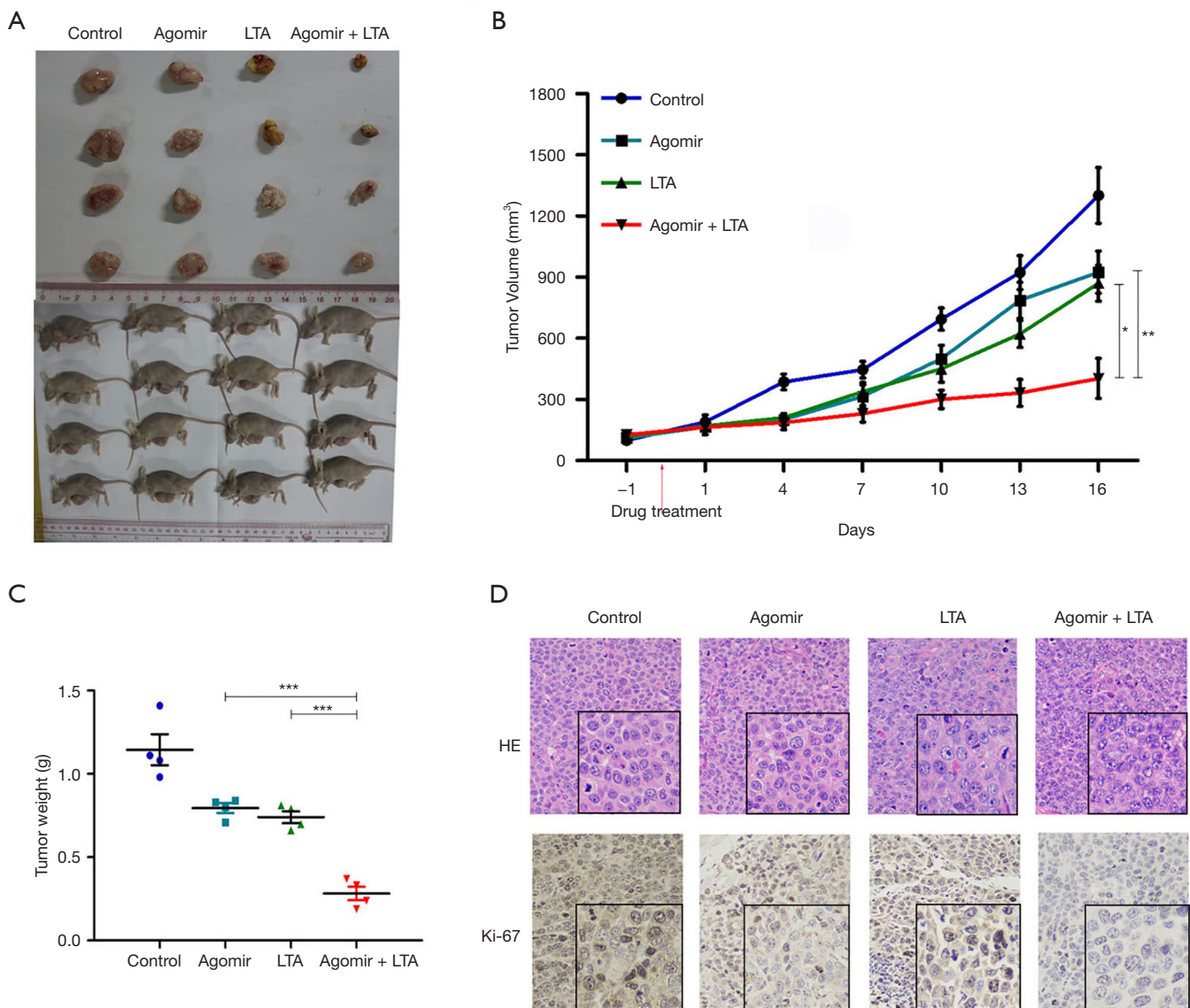
Figure 5 Combined use of lipoteichoic acid (LTA) and miR-27b-3p agomir has synergistic effect for anti-gastric cancer *in vivo*. Subcutaneous xenografts were established in nude mice, which were treated with miR-27b-3p agomir, LTA or together as indicated (n=4 per group). (A) The photos of tumor and mice are shown. The growth of tumor (B) was recorded and weight (C) is shown. (D) Hematoxylin-eosin staining of tumor tissues and Ki-67 immunohistochemistry analysis in xenograft tumor tissues were performed. ×400. All the experiments were carried out in triplicate. Magnification, 100×. *P<0.05, **P<0.01, ***P<0.001.

both poor disease-free and overall survival (30). The production of VEGFC was also induced by conventional or targeted radio- and chemo-therapy (31,32). VEGFC stimulated proliferation by promoting the phosphorylation of PI3K-AKT in spermatogonia GC-1 cells (33) and in N87 cells, the expression of VEGFC and VEGFD was significantly decreased by inhibition of p-Akt and p-mTOR pathways (23). Xiang *et al.* also reported that the expression of VEGFC was regulated by the PI3K/Akt pathway in colorectal cancer cells (28). Our results showed that decreased levels of VEGFC inhibited the phosphorylation of PI3K-AKT. We speculate that the decreased phosphorylation of PI3K-AKT will reduce the expression of VEGFC.

Previous studies have mainly demonstrated the immune regulatory effects of LTA and less attention has been paid to its preventive antitumor effect. LTA has been shown to inhibit melanogenesis in B16F10 mice (18) and its oral administration suppressed the growth of established skin tumors (17). However, LTA was also found to enhance the proliferation and metabolic activity of human non-small-cell lung cancer cells *in vitro* by activation of inflammatory signaling (34). Our data showed that LTA suppressed the proliferation of gastric cancer cells via regulating the NF-κB pathway. We suspect that this inconsistency in results may be due to differences in tumor cell types and the concentrations of LTA used in each experiment.

The NF-κB pathway supports cell survival and the acquisition of chemo resistance in gastric cancer (35-37). In LTA-induced murine macrophages, LTA was reported to activate NF-κB through the recognition of TLR2 and reactive oxygen species (26), and in LTA-induced endometritis mice, LTA promoted the activation of TLR2 and NF-κ (38). Immunofluorescence assay showed that the protein level of P65 in both the cytoplasm and nucleus of AGS cells was significantly decreased by treatment with LTA. Given the different cell types used and the disease being studied, more cancer cell lines might be explored in subsequent experiments. Different concentrations of LTA used to treat cancer cells might also be used.

MiR-27b-3p agomir showed a potent inhibition of tumor growth, and a synergistic inhibitory effect of miR-27b-3p agomir and LTA on gastric cancer was seen. Nowadays, miRNA agomir and miRNA inhibitors are considered promising therapeutics in the treatment of some cancers. However, the number of miRNA therapeutics progressing into clinical development is small because obstacles encountered in developing efficient delivery systems (39). The combination of miRNA therapeutics and other drugs is an intuitive strategy (40). However, drug candidates for miRNA therapeutics are also under investigation and their synergistic inhibitory effect needs to be explored.

The combined use of LTA and miR-27b-3p agomir showed a potent inhibition effect on the cell viability of AGS and more apoptosis cells compared to their individual effects. Our data preliminarily proposed combination therapy for anti-gastric cancer treatment using LTA and miR-27b-3p agomir. The combination of therapies we propose serves as a promising avenue for gastric cancer therapy. Although our studies have demonstrated the synergistic effects of combining LTA and miR-27b-3p

agomir, further studies are warranted to explore the optimal concentration of the two substances and the safety of this form of treatment.

Acknowledgments

Footnote

Reporting Checklist: The authors have completed the ARRIVE reporting checklist. Available at http://dx.doi.org/10.21037/jgo-21-12

Data Sharing Statement: Available at http://dx.doi.org/10.21037/jgo-21-12

Conflicts of Interest: All authors have completed the ICMJE uniform disclosure form (available at http://dx.doi.org/10.21037/jgo-21-12). The authors have no conflicts of interest to declare.

Ethical Statement: The authors are accountable for all aspects of the work in ensuring that questions related to the accuracy or integrity of any part of the work are appropriately investigated and resolved. Experiments were performed under a project license (NO.: IEC2020011600012) granted by Ethics Committee of the SSL Central Hospital of Dongguan City, in compliance with SSL Central Hospital of Dongguan City guidelines for the care and use of animals.

References

1. Huang J, Yang Y, Yang J, et al. Regenerating gene family member 4 promotes growth and migration of gastric cancer through protein kinase B pathway. Int J Clin Exp Med 2014;7:3037-44.

2. Wang J, Wang Q, Liu H, et al. MicroRNA expression and its implication for the diagnosis and therapeutic strategies of gastric cancer. Cancer Lett 2010;297:137-43.

3. Karimi P, Islami F, Anandasabapathy S, et al. Gastric cancer: descriptive epidemiology, risk factors, screening, and prevention. Cancer Epidemiol Biomarkers Prev 2014;23:700-13.

4. Jemal A, Bray F, Center MM, et al. Global cancer statistics. CA Cancer J Clin 2011;61:69-90.

5. Zhao JJ, Pan K, Wang W, et al. The prognostic value of tumor-infiltrating neutrophils in gastric adenocarcinoma after resection. PLoS One 2012;7:e33655.

6. Takahashi T, Saikawa Y, Kitagawa Y. Gastric cancer: current status of diagnosis and treatment. Cancers (Basel) 2013;5:48-63.

7. Abbas M, Faggian A, Sintali DN, et al. Current and future biomarkers in gastric cancer. Biomed Pharmacother 2018;103:1688-700.

8. Achen MG, McColl BK, Stacker SA. Focus on lymphangiogenesis in tumor metastasis. Cancer Cell 2005;7:121-7.

9. Bhat SA, Majid S, Rehman MU. Scenario and future prospects of microRNAs in gastric cancer: A review. Iran J Basic Med Sci 2019;22:345-52.

10. Link A, Kupcinskas J. MicroRNAs as non-invasive diagnostic biomarkers for gastric cancer: Current insights and future perspectives. World J Gastroenterol 2018;24:3313-29.

11. Feng Q, Wu X, Li F, et al. miR-27b inhibits gastric cancer metastasis by targeting NR2F2. Protein Cell 2017;8:114-22.

12. Chen X, Cui Y, Xie X, et al. Functional role of miR-27b in the development of gastric cancer. Mol Med Rep 2018;17:5081-7.

13. Tao J, Zhi X, Zhang X, et al. miR-27b-3p suppresses cell proliferation through targeting receptor tyrosine kinase like orphan receptor 1 in gastric cancer. J Exp Clin Cancer Res 2015;34:139.

14. Geng Y, Lu X, Wu X, et al. MicroRNA-27b suppresses Helicobacter pylori-induced gastric tumorigenesis through negatively regulating Frizzled7. Oncol Rep 2016;35:2441-50.

15. Shang Y, Feng B, Zhou L, et al. The miR27b-CCNG1-P53-miR-508-5p axis regulates multidrug resistance of gastric cancer. Oncotarget 2016;7:538-49.

16. Ginsburg I. Role of lipoteichoic acid in infection and inflammation. Lancet Infect Dis 2002;2:171-9.

17. Kim HR, Kim H, Jung BJ, et al. Lipoteichoic acid isolated from Lactobacillus plantarum inhibits melanogenesis in B16F10 mouse melanoma cells. Mol Cells 2015;38:163-70.

18. Friedrich AD, Campo VE, Cela EM, et al. Oral administration of lipoteichoic acid from Lactobacillus rhamnosus GG overcomes UVB-induced immunosuppression and impairs skin tumor growth in mice. Eur J Immunol 2019;49:2095-102.

19. Opal SM, Cohen J. Clinical gram-positive sepsis: does it fundamentally differ from gram-negative bacterial sepsis? Crit Care Med 1999;27:1608-16.

20. Schwandner R, Dziarski R, Wesche H, et al. Peptidoglycan- and lipoteichoic acid-induced cell activation is mediated by toll-like receptor 2. J Biol Chem 1999;274:17406-9.

21. Xie N, Wang Y, Wang Q, et al. Lipoteichoic acid of Bifidobacterium in combination with 5-fluorouracil inhibit tumor growth and relieve the immunosuppression. Bulletin Du Cancer 2012;99:E55-63.

22. Wu YR, Qi HJ, Deng DF, et al. MicroRNA-21 promotes cell proliferation, migration, and resistance to apoptosis through PTEN/PI3K/AKT signaling pathway in esophageal cancer. Tumour Biol 2016;37:12061-70.

23. Chen H, Guan R, Lei Y, et al. Lymphangiogenesis in gastric cancer regulated through Akt/mTOR-VEGF-C/VEGF-D axis. BMC Cancer 2015;15:103.

24. Wang Y, Xing QF, Liu XQ, et al. MiR-122 targets VEGFC in bladder cancer to inhibit tumor growth and angiogenesis. Am J Transl Res 2016;8:3056-66.

25. Yu Y, Yu J, Pei CG, et al. Xanthatin, a novel potent inhibitor of VEGFR2 signaling, inhibits angiogenesis and tumor growth in breast cancer cells. Int J Clin Exp Pathol 2015;8:10355-64.

26. Zhao G, Jiang K, Wu H, et al. Polydatin reduces Staphylococcus aureus lipoteichoic acid-induced injury by attenuating reactive oxygen species generation and TLR2-NFkappaB signalling. J Cell Mol Med 2017;21:2796-808.

27. Rauniyar K, Jha SK, Jeltsch M. Biology of Vascular Endothelial Growth Factor C in the Morphogenesis of Lymphatic Vessels. Front Bioeng Biotechnol 2018;6:7.

28. Xiang L, Xie G, Ou J, et al. The extra domain A of fibronectin increases VEGF-C expression in colorectal

carcinoma involving the PI3K/AKT signaling pathway. PLoS One 2012;7:e35378.

29. Pepper MS. Lymphangiogenesis and tumor metastasis: myth or reality? Clin Cancer Res 2001;7:462-8.

30. Petrillo A, Laterza MM, Tirino G, et al. Increased circulating levels of vascular endothelial growth factor C can predict outcome in resectable gastric cancer patients. J Gastrointest Oncol 2019;10:314-23.

31. Dufies M, Giuliano S, Ambrosetti D, et al. Sunitinib Stimulates Expression of VEGFC by Tumor Cells and Promotes Lymphangiogenesis in Clear Cell Renal Cell Carcinomas. Cancer Res 2017;77:1212-26.

32. Lupu-Plesu M, Claren A, Martial S, et al. Effects of proton versus photon irradiation on (lymph)angiogenic, inflammatory, proliferative and anti-tumor immune responses in head and neck squamous cell carcinoma. Oncogenesis 2017;6:e354.

33. Zhao L, Zhu Z, Yao C, et al. VEGFC/VEGFR3 Signaling Regulates Mouse Spermatogonial Cell Proliferation via the Activation of AKT/MAPK and Cyclin D1 Pathway and Mediates the Apoptosis by affecting Caspase 3/9 and Bcl-2. Cell Cycle 2018;17:225-39.

34. Hattar K, Reinert CP, Sibelius U, et al. Lipoteichoic acids from Staphylococcus aureus stimulate proliferation of human non-small-cell lung cancer cells in vitro. Cancer Immunol Immunother 2017;66:799-809.

35. Endo F, Nishizuka SS, Kume K, et al. A compensatory role of NF-kappaB to p53 in response to 5-FU-based chemotherapy for gastric cancer cell lines. PLoS One 2014;9:e90155.

36. Maeda S, Omata M. Inflammation and cancer: role of nuclear factor-kappaB activation. Cancer Sci 2008;99:836-42.

37. Neumann M, Naumann M. Beyond IkappaBs: alternative regulation of NF-kappaB activity. FASEB J 2007;21:2642-54.

38. Jiang K, Guo S, Yang J, et al. Matrine alleviates Staphylococcus aureus lipoteichoic acid-induced endometritis via suppression of TLR2-mediated NF-kappaB activation. Int Immunopharmacol 2019;70:201-7.

39. Lai X, Eberhardt M, Schmitz U, et al. Systems biology-based investigation of cooperating microRNAs as monotherapy or adjuvant therapy in cancer. Nucleic Acids Res 2019;47:7753-66.

40. Jonas S, Izaurralde E. Towards a molecular understanding of microRNA-mediated gene silencing. Nat Rev Genet 2015;16:421-33.